

Joint Optimization of 3D Placement and Radio Resource Allocation for per-UAV Sum Rate Maximization

Asad Mahmood, Thang X. Vu, *Senior Member, IEEE*, Symeon Chatzinotas, *Fellow, IEEE*,
Björn Ottersten, *Fellow, IEEE*,

Abstract—Unmanned aerial vehicles (UAV) have emerged as a practical solution that provides on-demand services to users in areas where the terrestrial network is non-existent or temporarily unavailable, e.g., due to natural disasters or network congestion. In general, UAVs’ user-serving capacity is typically constrained by their limited battery life and the finite communication resources that highly impact their performance. This work considers the orthogonal frequency division multiple access (OFDMA) enabled multiple unmanned aerial vehicles (multi-UAV) communication systems to provide on-demand services. The main aim of this work is to derive an efficient technique for the allocation of radio resources, 3D placement of UAVs, and user association matrices. To achieve the desired objectives, we decoupled the original joint optimization problem into two sub-problems: (i) 3D placement and user association and (ii) sum-rate maximization for optimal radio resource allocation, which are solved iteratively. The proposed iterative algorithm is shown via numerical results to achieve fast convergence speed after fewer than 10 iterations. The benefits of the proposed design are demonstrated via superior sum-rate performance compared to existing reference designs. Moreover, results showed that the optimal power and sub-carrier allocation help to mitigate the inter-cell interference that directly impacts the system’s performance.

Index Terms—5G, multi UAV communication, convex optimization, internet of things (IoT).

I. INTRODUCTION

THE 5G communication system aims to provide massive connectivity, ultra-reliable low-latency communication, and ensure the end-user quality of service. In contrast, according to [2], [3], terrestrial networks have not yet covered most remote areas due to the sparse human activities in these regions. Similarly, the goal of providing massive connectivity services is highly compromised in the case of an emergency where the existing communication system is disrupted due to natural disasters or faces congestion caused by the temporal increment in the number of users. Moreover, the excessive demand for the users’ resources and connectivity represents a challenging task in meeting the objectives mentioned earlier [4]. To overcome the above-mentioned challenges, different solutions have been proposed, e.g., device-to-device communication (D2D), to provide a wide range of communication

services that allow devices in the vicinity of each other to communicate without relaying account the base station (BS). However, due to the adverse nature of wireless communication channels in emergency scenarios, it is challenging to optimize the route between the users [5]. Second, satellite communication emerges as an effective solution for providing on-demand communication services to users in emergency scenarios, despite the low data rate and high latency that act as bottlenecks for widespread adoption, e.g., GEO satellites. [6]. Furthermore, due to characteristics such as flexibility, adaptive altitude, and effortless deployment, unmanned aerial vehicles (UAVs) are emerging as an effective solution for providing reliable communication services to a user located in a particular location [4].

UAVs, colloquially referred to as drones or flying base stations (BSs), have gained substantial attention in academia and industries, with applications ranging from photography to search and rescue operations, package delivery, agriculture, and other real-time applications [7]. One of the promising but challenging tasks in UAV communication systems is determining how to deploy UAVs to provide massive coverage to user equipment (UEs) while meeting quality of service (QoS) requirements and improving network energy efficiency [8]. Due to limited battery capacity, it should be carefully considered when designing the UAV deployment plan, together with other issues such as security, privacy, and flight regulations [9]. In multi-UAV systems, the placement problem is more challenging to guarantee a balanced trade-off between shadowing, path loss, and interference. Recent studies show that an increase in the altitude of UAVs leads to an increase in the probability of line-of-sight communication; in contrast, it also adds additional path loss [10]. Hence, considering the joint UAV deployment in 3D cartesian coordinates and resource allocation is of great importance to enhance the UAV communication systems in emergency scenarios. Based on the above motivation, this work focuses on the joint 3D placement and resource allocation to improve the power efficiency of the multi-UAV network. The following subsection studies related works on UAV communication, followed by the main contributions of this paper.

A. Related Works

The study on the UAV placement problem has recently been investigated in both 2D [11]–[14] and 3D [15], [16] cartesian coordinates. By employing a UAV as a relying node, the sum rate of the two-way relaying network can be improved via a joint optimization of the UAV trajectory and resource

This work was supported by the Luxembourg National Research Fund via project 5G-Sky, ref. FNR/C19/IS/13713801/5G-Sky, and project RUTINE, ref. FNR/C22/IS/17220888/RUTINE.

The part of this work has been accepted for publication at the IEEE VTC2023-Spring, Italy [1]

The authors are with the Interdisciplinary Centre for Security, Reliability and Trust (SnT), University of Luxembourg, 4365 Luxembourg City, Luxembourg. Email: {asad.mahmood, thang.vu, symeon.chatzinotas, bjorn.ottersten}@uni.lu.

allocation while assuring the user QoS requirements [11]. The authors of [12] considered a UAV-enabled wireless power communication network to maximize common throughput by optimizing the trajectory and communication resources simultaneously while taking the UAV's maximum speed and users' energy neutrality into account. In [13], the authors maximize the UAV communication network's average secrecy rate by designing an optimal path and transmission power control. To improve QoS and provide communication services to edge users, the authors of [14] considered an OFDMA-enabled UAV relay network. In [15], authors proposed a UAV placement algorithm to maximize served users using minimum transmission power. Furthermore, in [16], the authors considered a wireless sensor network scenario in which UAVs follow an optimal trajectory to maximize the data collection rate.

The works above optimize the UAV deployment for a single-UAV network, which may not be applicable in high-demand scenarios. In such cases, employing multiple UAVs simultaneously could significantly improve the system performance if the UAV placement, user association, and transmission power control are properly designed [2], [7], [17]–[20]. In multi-UAV systems, 3D placement design has been proven to be more efficient in terms of the sum rate than 2D placement via optimizing the UAVs' altitude to maximize the UAV's coverage and minimize inter-UAV interference [2], [17], [18]. Besides providing massive connectivity and ultra-reliable low-latency communication, energy efficiency and efficient utilization of resources are also essential performance metrics. To provide the same user demands, the smaller number of deployed UAVs is, the higher UAV utilization we have. The authors of [19] proposed a bisection-based algorithm to determine the minimum number of UAVs among candidate locations which can provide service to all IoT users. It is noted that no bandwidth or power allocation was considered therein. The authors of [20] maximized the average capacity by deploying a minimum number of UAVs while ensuring that deployed UAVs can cover all massive or scattered users. A similar approach was considered in [7], which minimizes the number of UAVs in a 3D coordinate for different system scenarios.

B. Contributions

This work studies the performance of an OFDMA-enabled multi-UAV system deployed to provide on-demand communication services to ground users. OFDMA is regarded as a promising candidate for the beyond 5G wireless networks due to its numerous benefits, such as flexible bandwidth and power allocation over users. [21]. Therefore, it fits well into our UAV-enabled wireless communication network to maximize the system sum rate and minimize the number of deployed UAVs while meeting given QoS requirements through joint optimization of 3D placement, sub-carrier allocation, and power control. The most related works in the literature to ours are presented in [14], [20]. In [14], a single OFDMA-based UAV acts as the relay to provide services to cell-edge users of a BS. Whereas in [20], a 2D-based UAV placement algorithm was proposed to maximize the average capacity of the UAV. It is noted that the solution in [20] does not consider

power and bandwidth allocation. Furthermore, [20] considers only the free-space LoS channel model, while we consider the practically probabilistic channel model. Our contributions are as follows:

- 1) We consider the joint design of the 3D placement, sub-carrier allocation, and power control for the per-UAV sum-rate maximization in the downlink OFDMA-enabled multi-UAV communications to serve users in areas where the existing communication network is highly compromised by congestion or natural disaster.
- 2) We formulate a joint optimization of 3D UAV placement, user association, sub-carrier allocation, and transmit power to maximize the system sum rate while deploying a minimum number of active UAVs. Due to the inherent non-convexity, the original problem is decoupled into two sub-problems: i) path loss minimization and ii) sum rate maximization, which is then iteratively solved to provide the (local) optimal solution to the original joint problem.
- 3) To solve the first sub-problem, we propose a heuristic algorithm to determine the minimum required UAVs based on the user demands and the ergodic capacity each UAV can provide, followed by an iteration algorithm to optimize the UAV 3D placement and user association. To tackle the non-convexity of the rate function in the second sub-problem, a successive convex approximation (SCA)-based iterative algorithm is proposed. In addition, a binary relaxation with a proper penalty function is implemented to accelerate the computation time. We show that the convergence to at least a local optimum of the proposed iterative algorithm is theoretically guaranteed.
- 4) The effectiveness of the proposed approach is demonstrated by the numerical results, which show a significant improvement in the number of served users, power efficiency, and sum rate when deploying a minimum number of UAVs while adhering to the quality of service constraint of each user.

C. Organization

The following sections summarize the rest of the paper: Section II summarizes the proposed system model and problem statement. Section III presented an algorithm for efficient 3D UAV deployment and resource allocation. Likewise, Section IV contains the simulation results. The paper is finally concluded in Section V

II. SYSTEM MODEL AND PROBLEM FORMULATION

In this work, we consider a down-link UAV-assisted wireless communication system that provides on-demand services to users in areas where the terrestrial network is non-existent or temporarily unavailable, e.g., due to natural disasters or network congestion, as shown in Fig. 1. The considered system model consists of M available UAVs equipped with U antennas and N users, which are represented by the sets $\mathcal{M} = \{1, 2, \dots, M\}$ and $\mathcal{N} = \{1, 2, \dots, N\}$, respectively. In order to improve UAVs' deployment usage, only $L \leq M$ UAVs will be activated to serve the users. The set of active

UAVs is denoted by $\mathcal{L} \subset \mathcal{M}$. We consider 3D coordinates, in which the location of the l -th UAV is represented by (x^l, y^l, h^l) , which satisfy:

$$\begin{cases} x_{\min} \leq x^l \leq x_{\max}, \forall l \\ y_{\min} \leq y^l \leq y_{\max}, \forall l \\ h_{\min} \leq h^l \leq h_{\max}, \forall l \end{cases} \quad (1)$$

where $(\cdot)_{\min}$ and $(\cdot)_{\max}$ represent the lower and upper bound of l -th UAV coordinates, respectively. The coordinates of the users are denoted by $\{x_n, y_n, 0\}$. For notation convenience, we denote $z^l \triangleq \{x^l, y^l\}$ and $v_n \triangleq \{x_n, y_n\}$ as the horizontal coordinates of l -th UAV and n -th UE. The UAVs are assisted by a central controller that provides information about UE's location [8]. The total users are divided into clusters, each of which will be served by one active UAV. In order to minimize interference, each UAV serves its connected users via OFDMA [14], which consists of K sub-channels denoted by $\mathcal{K} = \{1, \dots, K\}$. We note that although there is no intra-cluster interference, there exists inter-cluster interference caused by the transmission of neighbouring UAVs.

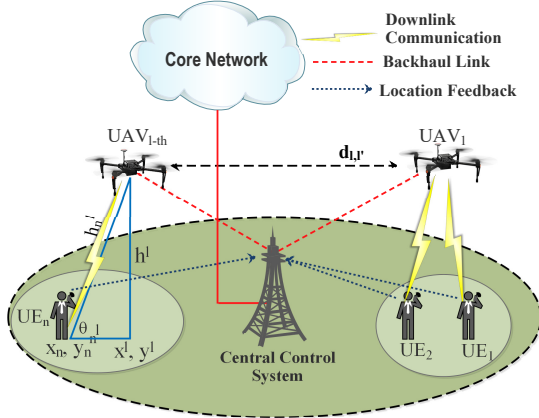


Fig. 1: System model.

Let us denote the sub-channel allocation matrix by $\mathbf{A} = [a_n^{k,l}]_{N \times K \times L}$, where $a_n^{k,l} = 1$ indicates that sub-channel k served by UAV l is allocated to user n and $a_n^{k,l} = 0$ otherwise. In addition, we denote $p_n^{k,l}$ as the transmit power from UAV l to user n over sub-channel k . Since UAV l only consumes power on sub-channel k for user n if that sub-channel is assigned to user n , we introduce the following constraint:

$$p_n^{k,l} \leq a_n^{k,l} P_t^{Max}, p_n^{k,l} \geq 0, a_n^{k,l} \in \{0, 1\}, \forall n, k, l. \quad (2)$$

where P_t^{Max} is the maximum transmit power of the UAV. The transmit power constraint (2) not only facilitates the rate function, as will be shown later in this section but also guarantees no transmit power on sub-channel k if it is not assigned to user n . To avoid mutual interference among the users, each sub-channel in one cluster (served by one UAV) is allocated to only one user, which imposes the following constraint:

$$\sum_{n \in \mathcal{N}} a_n^{k,l} \leq 1, \forall k, l. \quad (3)$$

Similarly, the user association $\mathbf{J} = [J_n^l]_{N \times L}$ is a binary matrix, in which each entity J_n^l represents the connection between l -th UAV and n -th UE, i.e., $J_n^l = 1$ if user n is

associated with UAV l , and $J_n^l = 0$ otherwise. Consequently, the following constraint must be met as one subchannel is only allocated to a user if it is connected to the corresponding UAV:

$$\sum_{k \in \mathcal{K}} a_n^{k,l} \leq J_n^l, J_n^l \in \{0, 1\}, \forall n, l. \quad (4)$$

A. Path Loss Model

We consider the general probabilistic channel modelling in which the channel between UAVs and their associated users includes both LOS and non-LOS (NLOS) parts. The probability of LoS is primarily determined by the 3D geographical location of UAVs and users on the ground, as well as the surrounding environment, as given below [15]:

$$P\text{Los}_n^l = \frac{1}{1 + b_1 \exp(-b_2(\theta_n^l - b_1))}. \quad (5)$$

In (5), b_1 and b_2 are the constants representing the environment condition, and $\theta_n^l = 180/(\pi \sin(h_l/d_n^l))$ is the angle of elevation between the l -th UAV and the n -th UE,

where $d_n^l = \sqrt{\|z^l - v_n\|^2 + h^l^2}$ is the distance between the l -th UAV and n -th user. The probability of non-line of sight (PNLoS) communication is represented by $P\text{NLoS}_n^l = 1 - P\text{Los}_n^l$.

The air-to-ground (A2G) path loss model of both LoS and NLoS between l -th UAV and n -th user is given as

$$P\hat{L}_n^l = \begin{cases} \xi_{LoS} K_o, & \text{for LoS} \\ \xi_{NLoS} K_o, & \text{for NLoS} \end{cases}, \quad (6)$$

where ξ_{NLoS} and ξ_{LoS} represent the attenuation factors for both NLoS and LoS links, respectively; $K_o = \left(\frac{4\pi f_c d_n^l}{c}\right)^\alpha$; f_c , α and c respectively represent the carrier frequency, path loss exponent and speed of light. Therefore, the UAV-User path loss is given as follows [22]:

$$P\text{L}_n^l = K_o \left[P\text{Los}_n^l \xi_{LoS} + \xi_{NLoS} P\text{NLoS}_n^l \right]. \quad (7)$$

B. Transmission Model

Let $\mathbf{h}_n^{k,l} \in \mathbb{C}^{U \times 1}$ be the small-scale fading from UAV l to user n on sub-channel k . To improve the receive SNR, we employ the maximum ratio transmission precoding, which results in an effective channel gain $g_n^{k,l} = |(\mathbf{h}_n^{k,l})^H \mathbf{h}_n^{k,l}|^2 / P\text{L}_n^l$, where $P\text{L}_n^l$ is given in (7). The downlink signal received on the k -th subchannel at user n from UAV l is given as follows:

$$y_n^{k,l} = \underbrace{\sqrt{p_n^{k,l}} g_n^{k,l} s_n^{k,l}}_{\text{Information signal}} + \underbrace{\sum_{l' \neq l} \left(\sum_{n' \neq n} \sqrt{p_{n'}^{k,l'}} g_{n'}^{k,l'} s_{n'}^{k,l'} \right) + n_n^k}_{\text{Inter-cell interference}}. \quad (8)$$

where $p_n^{k,l}$ and $s_n^{k,l}$ represent the transmission power of l -th UAV and information transmitted signal with $\mathbb{E}|s_n^{k,l}|^2 = 1$, respectively, and n_n^k is the Gaussian noise with zero mean and variance σ^2 . The first term on the right-hand side of (8) represents the information signal transmitted over the sub-carrier k by the l -th UAV to the n -th user. The second term represents the interference caused by other UAVs' transmission on the same sub-carrier k . Therefore, the signal-to-interference plus

noise ratio (SINR) of sub-channel k of at user n from UAV l is given as

$$\gamma_n^{k,l} = p_n^{k,l} g_n^{k,l} / (\Phi_n^{k,l} + \sigma^2), \quad (9)$$

where $\Phi_n^{k,l} = \sum_{l' \neq l} \left(\sum_{n' \neq n} p_{n'}^{k,l'} \right) g_n^{k,l'}$ is the aggregated interference imposed by other UAVs. Thus, the achievable rate of n -th UE connected to l -th UAV is calculated as

$$R_n^l = B \sum_{k \in \mathcal{K}} \log_2 (1 + \gamma_n^{k,l}). \quad (10)$$

C. Problem Formulation

Unlike previous works, which target only the sum-rate maximization, we also optimize the system-wise energy usage. Therefore, our objective is to maximize the ratio between the system sum rate and the number of active UAVs, which is given as $\Upsilon = \frac{R_{sum}}{L} = \frac{\sum_{n,l} R_n^l}{L}$, where R_n^l is calculated in (10), and L is the number of active UAVs. We aim to jointly optimize the UAVs' 3D placement, user association, power and subcarrier allocation to maximize the objective function Υ . For ease of presentation, we introduce short-hand notations $\mathbf{W} = [W^l \triangleq x^l, y^l, h^l]$, $\mathbf{P} = [p_n^{k,l}]_{N \times K \times L}$, $\mathbf{J} = [J_n^l]_{N \times L}$, and $\mathbf{A} = [a_n^{k,l}]_{N \times K \times L}$. Furthermore, let us denote r_{0n} as the QoS requirement of user n , and C_{Min}^l, C_{Max}^l as the minimum and maximum numbers of users the UAV can serve, respectively. Then the joint optimization is formulated as follows:

$$\mathbb{P}_0 : \max_{L, \mathbf{W}, \mathbf{P}, \mathbf{J}, \mathbf{A}} \frac{1}{L} \sum_{l \in \mathcal{L}} \sum_{n \in \mathcal{N}} R_n^l \quad (11a)$$

$$\text{s.t. Equations (1) to (4)}. \quad (11b)$$

$$R_n^l \geq J_n^l r_{0n}, \forall n, l, \quad (11c)$$

$$\sum_{l \in \mathcal{L}} J_n^l \leq 1, \forall n, \quad (11d)$$

$$\sum_{n \in \mathcal{N}} J_n^l \in [C_{Min}^l, C_{Max}^l], \forall l, \quad (11e)$$

$$\sum_{n \in \mathcal{N}} \sum_{k \in \mathcal{K}} p_n^{k,l} \leq P_t^{Max}, \forall l, \quad (11f)$$

$$\sum_{n \in \mathcal{N}} \sum_{l \in \mathcal{L}} J_n^l \geq \lambda N, \quad (11g)$$

$$\|\mathbf{W}^l - \mathbf{W}^{l'}\| \geq d_o, \forall l. \quad (11h)$$

Our objective in this work is to deploy a minimum number of UAVs to maximize the average serving rate, subject to QoS and system resource requirements. In problem \mathbb{P}_0 , constraint (11c) ensures the QoS requirement of corresponding UE-UAV link; (11d) guarantees that no UE is connected to more than one UAV; (11e) represents the bounds of the serving capacity of each UAV; (11f) restricts the total transmit power at each UAV should not exceed the maximum power; (11g) guarantees the minimum λ per cent of the UEs should be served; finally, (11h) constraints the distance between the two neighbouring UAVs not exceeding the minimum allowable distance to avoid a collision. Note that by setting λ equals to 1, constraints (11g) together with (11c) assure the QoS requirements for all users.

III. FRAMEWORK FOR OPTIMAL 3D PLACEMENT, USER ASSOCIATION, AND RADIO RESOURCE ALLOCATION

The optimization problem in (11) is mixed-integer non-linear programming (MINLP) and NP-hard due to the integer

nature of the user association matrix \mathbf{J} , and sub-carrier allocation matrix \mathbf{A} . Furthermore, it is challenging to get optimal results as it involves non-linear, non-convex objective function and constraints. Towards an efficient solution to problem \mathbb{P}_0 in (11), we decouple the original optimization problem into two sub-problems: i) the first sub-problem, denoted by \mathbb{P}_1 , optimizes the number of active UAVs, their optimal 3D placement, and the user association to minimize the average path loss; ii) and the second sub-problem, denoted by \mathbb{P}_2 , optimizes the radio resources (power and subcarrier allocation) to minimize inter-cell interference and maximize the sum rate of users. In the following, we will detail the sub-problems, whose overview diagram of the problem decomposition is shown in Fig. 2.

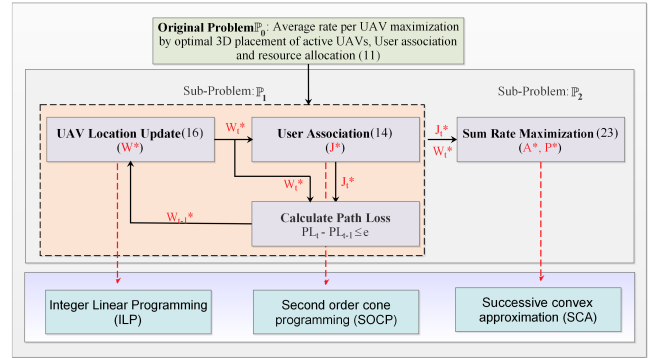


Fig. 2: Road-map of iterative algorithms.

A. Solving \mathbb{P}_1 : Optimal 3D Placement and User Association

The first sub-problem is directly obtained from the original problem by treating the radio resources (\mathbf{A} and \mathbf{P}) as constants, which is formulated as follows:

$$\mathbb{P}_1 : \max_{L, \mathbf{W}, \mathbf{J}} \frac{1}{L} \sum_{l \in \mathcal{L}} \sum_{n \in \mathcal{N}} R_n^l \quad (12)$$

s.t. Equations (1), (4), (11c) to (11e), (11g) and (11h).

Jointly optimizing the number of active UAVs, their 3D locations, and user association is challenging. To address this issue, we initially present a practical and effective heuristic approach to determine the optimal number of required UAVs denoted by L . Intuitively, L should depend on factors such as the number of ground users, the QoS requirements, and the average capacity of the networks [23]. By employing Shannon's capacity bound, the average spectral efficiency of any arbitrary user can be calculated as follows:

$$\Lambda = \mathbb{E} \left[\log_2 \left(1 + \frac{P_t^{max}}{f_c \sigma^2} \left(\frac{\mathbf{h}^H \mathbf{h}}{PL} \right)^2 \right) \right]. \quad (13)$$

Based on equation (7), the path loss is primarily determined by the LoS channel, which is dependent on the 3D geographical locations of the UAVs. We assume that the UAVs are positioned in a manner that ensures LoS dominance, i.e., $PLos \simeq 1$. Hence, the maximum data rate that a user can achieve over the bandwidth B is represented by $R^{max} = B \times \Lambda$. To satisfy the QoS requirement r_{0n} , the maximum number of user equipment (UEs) that each UAV can support is given by

$C^{\max} = \left\lceil \frac{R^{\max}}{r_{0n}} \right\rceil, \forall n$. Consequently, we employ a heuristic approach to determine the number of active UAVs denoted by $L = \left\lceil \frac{\lambda N}{C^{\max}} \right\rceil$, where λ denotes the percentage of users that need to be served. Let \mathcal{L} represent the set of active UAVs.

Once the number of active UAVs L is determined, the sub-problem \mathbb{P}_1 focuses on optimizing the placement of active UAV's in 3D space and their user associations. The altitude of each UAV is a critical factor in determining the probability of the line-of-sight (LoS) channel $PLos_n^l$. As the altitude of the UAV increases, so does the angle of elevation (θ_n^l), resulting in an increase in the value of $PLos_n^l$. However, higher altitude also leads to greater path losses between the UAV and its associated users, resulting in reduced sum rate [24]. Thus, the primary objective of the first sub-problem is to minimize path losses. To achieve this goal, the UAVs should be placed in locations where the probability of LoS communication is greater than or equal to a threshold value ϕ , i.e., $PLos_n^l(\theta_n^l) \geq \phi$. Additionally, each user should only be associated with the UAV located at a distance less than $h^l / \sin(PLos_n^l(\phi))$.

1) *User Association*: Based on the above analysis, we propose to solve the first sub-problem via an alternative optimization algorithm, which treats each of the UAVs' locations and the user association matrix independently, assuming the other is fixed. Therefore, we model an iterative mathematical framework for optimal 3D placement and user association to minimize the path loss between the UAVs and their associated users. Following that, the UEs association problem, given the location of UAVs and UEs, can be formulated as follows:

$$\mathbb{P}_1^a : \min_{\mathbf{J}} \sum_{n \in \mathcal{N}} \sum_{l \in \mathcal{L}} J_n^l \|\mathbf{V}_n - \mathbf{W}_l\|^2 \quad (14a)$$

$$\text{Equations (11d), (11e) and (11g),} \quad (14b)$$

$$J_n^l \|\mathbf{V}_n - \mathbf{W}_l\| \leq \frac{h_l}{\sin(PLos_n^l(\phi))}, \forall n, l. \quad (14c)$$

where $\mathbf{V}_n \triangleq (x_n, y_n, 0)$ represents the location of user n . The optimization problem mentioned in (14) is integer linear programming and convex in nature and can be solved using the standard methods, e.g., integer linear programming (ILP).

2) *UAV's Location*: Given the user association matrix \mathbf{J} calculated in problem (14), the location of the UAV is updated such that the distance between the UAV and associated UEs is minimized. Denote $Q^l \in \mathcal{Q}$ as the number of UEs associated with the l -th UAV, the UAVs' 3D placement problem can be formulated as follows:

$$\mathbb{P}_1^b : \min_{\mathbf{W}} \sum_{n \in Q^l} \left[(x_n - x_l)^2 + (y_n - y_l)^2 + h_l^2 \right], \forall l, \quad (15a)$$

$$(x_n - x_l)^2 + (y_n - y_l)^2 + h_l^2 \xi \leq 0, \forall n \in Q^l, \quad (15b)$$

$$\text{Equations (1) and (11h).} \quad (15c)$$

The parameter $\xi = 1 - 1/\sin(PLos_n^l(\phi))$ is introduced in constraint (15b) to ensure that the UAV is placed at the point where the angle of elevation calculated based on its geographical location should satisfy $PLos_n^l(\theta_n^l) \geq \phi$. Because the objective function and the first constraint are both quadratic, hence (15) is a quadratic constraint quadratic

Algorithm 1: Iterative Algorithm to solve (14) and (16)

```

1 Initialization:  $PL_{old}$ , error;
2 Execution: ;
3 while error >  $\epsilon$  do
4   Given the random location of UAV's Solve (14) Using
   Branch and Bound (BnB) algorithm to get the User
   association matrix  $\mathbf{J}$ .
5   Based upon the User Association matrix, update the
   location of UAV by solving (15)
6   Compute Path Loss using using (7) to obtain  $PL_*$ 
7   Compute error =  $|PL_* - PL_{old}|$ 
8   Update  $PL_{old} = PL_{old} - PL_*$ 
9 end

```

programming problem (QCQP). *Lemma 1*: Problem (15) can be equivalently formulated as a following QCQP problem:

$$\mathbb{P}_1^{b,1} : \min_{\mathbf{W}} \frac{1}{2} \mathbf{W}^T \mathbf{H}_o \mathbf{W} + \mathbf{F}_o^T \mathbf{W} + \kappa_o, \forall l \quad (16a)$$

$$\frac{1}{2} \mathbf{W}^T \mathbf{H}_n + \mathbf{F}_n^T \mathbf{W} + \kappa_n \leq 0, \forall n \in Q^l. \quad (16b)$$

Where

$$\mathbf{H}_o = \begin{bmatrix} 2Q^l & 0 & 0 \\ 0 & 2Q^l & 0 \\ 0 & 0 & 2Q^l \end{bmatrix}, \mathbf{H}_n = \begin{bmatrix} 2 & 0 & 0 \\ 0 & 2 & 0 \\ 0 & 0 & \xi \end{bmatrix}. \quad (17)$$

$$\mathbf{F}_o = \left[-2 \sum_{n \in Q^l} x_n \quad -2 \sum_{n \in Q^l} y_n \quad 0 \right]^T, \mathbf{F}_n = \left[-2x_n \quad 0y_n \quad 0 \right]^T. \quad (18)$$

$$\kappa_o = \sum_{n \in Q^l} x_n^2 + \sum_{n \in Q^l} y_n^2, \quad \kappa_n = x_n^2 + y_n^2. \quad (19)$$

Proof: See Appendix A. ■

Solving a QCQP optimization, in general, is challenging because of its NP-hard nature [25]. Fortunately, there is a subclass of QCQP problems in which both the objective function and constraint are convex in nature, as demonstrated in (17). This subclass of problems can be efficiently solved using the second-order cone programming method [26].

By iteratively solving problems (16) and (14), the average path loss and the user association can be optimized, whose steps are listed in Algorithm 1.

3) *Convergence and Complexity Analysis of Algorithm 1*:

a) *Convergence Analysis*:

$$\mathbb{F}(\mathbf{W}^{t+1}) \leq \mathbb{F}(\mathbf{W}^t), \quad \mathbb{F}(\mathbf{J}^{t+1}) \leq \mathbb{F}(\mathbf{J}^t). \quad (20)$$

Equation (20) perceives that the objective function values of (14) and (16) decrease as with the iterations; as a result path loss $PL(\mathbf{W}, \mathbf{J})$ starts decreasing and converges to a finite value when the difference between the current and previous iteration is less than epsilon ϵ , i.e., $PL^t - PL^{t-1} \leq \epsilon$.

b) *Complexity Analysis*: This section provides the per iteration worst-case complexity analysis of Algorithm 1 that solves (14) and (16) iteratively. Since the (14) is the least square minimization problem and convex in nature, it can be solved efficiently using integer programming. More specifically, a convex problem (14) involves NL decision variables and $2NL + 2L + 2L + 1$ constraints. Because of this, we can express $(NL)^3(2NL + 2L + 2L + 1)$ as the complexity required to solve (14) in each iteration. On

the other hand, in optimization problem (16), compromise of $3Q^l$ decision variables and $Q^l + 7L$ constraints. Likewise, to solve (16), the required per-iteration complexity is $(3Q^l)^{0.5} (Q^l + 7L)$. Furthermore, assuming that t_m are a total number of iterations, the total complexity of Algorithm 1 is $\mathcal{O} \left(t_m \left((NL)^3 (2NL + 2L + 2L + 1) + (3Q^l)^{0.5} (Q^l + 7L) \right) \right)$.

B. Solving \mathbb{P}_2 : Joint Optimization of Transmit Power and Subcarrier Allocation

Once the UAVs' location and the user association matrix are defined, the second subproblem will jointly optimize the transmit power at the UAVs and the subcarrier allocation to maximize the sum rate while guaranteeing users' QoS. Mathematically, the second subproblem is formulated as follows:

$$\mathbb{P}_2^a : \max_{\mathbf{P}, \mathbf{A}} \sum_{n \in \mathcal{N}} \sum_{l \in \mathcal{L}} R_n^l \quad (21a)$$

$$R_n^l \geq J_n^l r_{0n}, \forall n \in \mathcal{N}, l \in \mathcal{L}, \quad (21b)$$

$$\text{Equations (2) to (4) and (11f)}. \quad (21c)$$

where R_n^l is given in (10). The problem (21) is non-convex in nature due to R_n^l in objective function and constraint (21b). To tackle this difficulty, we introduce auxiliary variables $\eta_n^l, s_n^{k,l}, \forall n, l$ and reformulate (21) as

$$\mathbb{P}_2^{a,1} : \max_{\mathbf{A}, \mathbf{P}, \eta, s} \sum_{n \in \mathcal{N}} \sum_{l \in \mathcal{L}} \eta_n^l \quad (22a)$$

$$\sum_{k \in \mathcal{K}} \log(\Phi_n^{k,l} + \delta^2 + p_n^{k,l} g_n^{k,l}) \geq \frac{\log(2)\eta_n^l}{B} \quad (22b)$$

$$+ \sum_{k \in \mathcal{K}} s_n^{k,l}, \forall n \in \mathcal{N}, l \in \mathcal{L},$$

$$\Phi_n^{k,l} + \delta^2 \leq e^{s_n^{k,l}}, \forall n, l, k, \quad (22c)$$

$$\eta_n^l \geq J_n^l r_{0n}, \forall n \in \mathcal{N}, l \in \mathcal{L}, \quad (22d)$$

$$\text{Equations (2) to (4) and (11f)}. \quad (22e)$$

where (22d) guarantee the QoS requirement, and (22b) and (22c) equivalently represent $R_n^l \geq \eta_n^l$. Solving (22) is still challenging due to the non-convex constraint (22c). Fortunately, it has a form of different-of-convex (DC) constraint; hence we can employ the first-order approximation to convexify the right-hand-side of (22c), which can be reformulated as follows:

$$\mathbb{P}_2^{a,2} : \max_{\mathbf{A}, \mathbf{P}, \eta, s} \sum_{n \in \mathcal{N}} \sum_{l \in \mathcal{L}} \eta_n^l \quad (23a)$$

$$\Phi_n^{k,l} + \delta^2 \leq e^{s_{o_n}^{k,l}} (s_n^{k,l} - s_{o_n}^{k,l} + 1) \quad (23b)$$

$$\forall n \in \mathcal{N}, k \in \mathcal{K}, l \in \mathcal{L},$$

$$\text{Equations (2) to (4), (11f), (22b) and (22d)}. \quad (23c)$$

where $s_{o_n}^{k,l}$ is a feasible point of constraint (23b). Since the objective is linear and all constraints are either convex or linear with binary variables $a_n^{k,l}$, problem (23) can be solved by the standard branch-and-bound method via, e.g., Mosek solver. This method, however, incurs exponential complexity with the problem size. Therefore, we relax the binary variables into continuous ones. In addition, a penalty function $\Psi_n^l = \sum_{k \in \mathcal{K}} ((a_n^{k,l})^2 - a_n^{k,l})$ is added to the original objective function to promote the convergence. However, since Ψ_n^l is

Algorithm 2: Iterative Algorithm to solve (21)

```

1 Initialization:  $s_o, \eta_{old}$ , error;
2 Execution: ;
3 while error >  $\epsilon$  do
4   Given the location of UAVs and user association matrix
   form Algorithm 1, Solve (23) to get the optimal value
   of  $\eta_*, a_*, p_*, s_*$ 
5   Compute error =  $|\eta_* - \eta_{old}|$ 
6   Update  $\eta_{old} = \eta_*, s_o = s_*$ 
7 end

```

TABLE I: Environment values. H-RB: High-Rise Buildings [3]

Environment	Sub-Urban	Urban	Dense-Urban	H-RB
ξ_{LoS}	1	1	1.6	2.3
ξ_{NLoS}	21	20	23	34
b_1	4.88	9.61	12.08	27.23
b_2	0.43	0.16	0.11	0.08

convex, it cannot be added to the objective function. In order to accomplish this, we employ its first-order approximation, computed as

$$\Psi_n^l = \sum_{k \in \mathcal{K}} (2a_{o,n}^{k,l} a_n^{k,l} - (a_{o,n}^{k,l})^2 - a_{o,n}^{k,l}). \quad (24)$$

By using (24) as the approximated penalty function, a relaxed resource allocation optimization problem with penalty parameter μ can be formulated as follows:

$$\mathbb{P}_2^b : \max_{\mathbf{A}, \mathbf{P}, \eta, s} \sum_{n \in \mathcal{N}} \sum_{l \in \mathcal{L}} (\eta_n^l + \mu \Psi_n^l) \quad (25a)$$

$$0 \leq a_n^{k,l} \leq 1, \quad (25b)$$

$$\text{Equations (2) to (4) and (11f)}, \quad (25c)$$

$$\text{Equations (22b), (22d) and (23b)}.$$

It is observed that problem (25), which is the relaxed version of (23), is convex in nature because of the linear objective function and convex constraints. Thus, problem (25) can be solved efficiently using standard methods, e.g., the interior point. We note that problem (25) provides a (sub) optimal solution to problem (23) since it satisfies all constraints of this problem. In order to narrow the gap to the optimal solution of problem (23), an iterative Algorithm 2, constitute a sequence of convex optimization problems, is proposed. The key idea behind Algorithm 2 is to have better values of feasible variables in the approximated optimization problem.

1) *Initialization:* Algorithm 2 works iteratively to find the optimal solution; for this, they need initial values for the inner approximation of (23b). Furthermore, in an iterative algorithm, the feasibility of the solution is primarily determined by the initialization step. The most common approach to find the initial value for inner approximation is to solve the feasible problem, i.e., (23), without the objective function so that the solution satisfies all of the constraints mentioned. However, it is unattainable because of constraint (23b), as directly solving (23) also requires inner approximation, which is again an iterative process. Therefore, to determine the feasible initial value of s_o , we solve the left-hand side of (23b) with equal power transmission and by heuristically adjusting the subcarrier allocation matrix to satisfy the constraints in (2),(3) and

TABLE II: Simulations Parameters

Parameters	Values	Parameters	Values
N	10 - 50 users	ϕ	55% - 95%
K	8	r_{0n}	1 Mbps
B	20MHz	N_o	-170 dBm/Hz
α	4	f_c	900 MHz
h_{min}, h_{max}	21m, 100m	P_t^{Max}	0.2W

(4). This solution's output is referred to as the initial value of 5.

2) Convergence and Complexity Analysis of Algorithm 2:

a) *Convergence Analysis:* Denote $\mathbf{\Pi} = (\mathbf{A}^*, \mathbf{P}^*, \eta^*, \mathbf{s}^*)$ as the optimal solution to problem (23) at iteration t . Furthermore, the objective functions of the original (21) and approximated (23) optimization problem are represented by $\mathbb{F}_1(\mathbf{\Pi})$ and $\mathbb{F}_2(\mathbf{\Pi})$, respectively. Because the approximated problem's feasible region is a subset of the original optimization problem's feasible region, we have $\mathbb{F}_1(\mathbf{\Pi}) \geq \mathbb{F}_2(\mathbf{\Pi}), \forall \mathbf{\Pi}$. Furthermore, the objective function value of 3 improves iteratively, i.e., $\mathbb{F}(\mathbf{\Pi}^{t+1}) \geq \mathbb{F}(\mathbf{\Pi}^t)$, according to the authors in [27]. The objective function value is bounded by transmission power and QoS constraints and will converge to a local optimal solution. Although it does not guarantee the global optimal solution, where the performance gap to achieve the global optimal solution is left for future work.

b) *Complexity Analysis:* The complexity of Algorithm 2 is determined in this section by considering the number of decision variables and constraints in optimization problem (23). Since optimization problem (23) is convex, the interior-point method is applied to find the efficient solution. Specifically, $3NKL + NL$ decision variables and $8NKL + 5NL + KL + L$ constraints in convex problem (23) results in the per iteration complexity $\mathcal{O}((3NKL + NL)^3(8NKL + 5NL + KL + L))$ [28], [29]. Furthermore, assuming that t_m are a total number of iterations, the overall complexity of Algorithm 2 is $\mathcal{O}(t_m((3NKL + NL)^3(8NKL + 5NL + KL + L)))$.

IV. RESULTS AND DISCUSSION

This section demonstrates the effectiveness of the proposed algorithm via extensive Monte-Carlo simulations using the simulation parameter listed in Table II. In our simulations, the N users are distributed randomly across a $1\text{Km} \times 1\text{Km}$ area. Furthermore, UAVs are deployed to provide communication services using the OFDMA protocol. Depending on the communication environment, Table I lists additional attenuation coefficients for path loss (ξ_{LoS}, ξ_{NLoS}) and parameters (b_1, b_2) related to the probability of line-of-sight communication. Furthermore, the performance of the proposed scheme is evaluated for different KPIs, e.g., path loss and sum rate. In addition, the numerical results for path loss and sum rate are compared to the respective benchmark schemes.

In the first section of the proposed framework, optimal 3D placement and user association were achieved by iteratively solving the (16) and (14). The goal of path loss minimization is achieved, as described in Section III-A, by selecting the L number of active UAVs while taking into account the total

number of ground users, network average capacity and users' QoS requirements, e.g., constraint (11c). Furthermore, the proposed design is compared with the following references:

- *K-Mean Clustering:* This scheme employs the K -Mean clustering algorithm to partition the N number of users into L clusters. The location of centroids is regarded as the 2D location of the UAVs.
- *K-Medioid Clustering:* This scheme is used K -Medioid clustering algorithm to cluster the N number of users into the L distant set.
- *Mean-Shift Clustering:* The Mean-Shift clustering algorithm determines the 2D location of UAVs using the Mean-shift algorithm, which works on the principle of kernel density estimation function.
- *Random Association:* In this scheme, L number of UAVs are optimally deployed using (16), while users are randomly assigned to the UAVs.
- *Random Deployment:* In scheme, L number of UAVs are distributed randomly over an area, whereas the user are allocated to the UAVs using (14)

After determining the optimal 3D location of the UAVs and the users' association matrix, an efficient resource allocation problem (23) is solved to achieve the maximum sum rate that satisfies the QoS. Moreover, to demonstrate the *Proposed Scheme's* advantages for sum rate maximization, we compared the results to the following relevant benchmark schemes:

- *Ref. [1]:* In this scheme, optimal UAV locations and user association matrices are calculated by solving (16) and (14), respectively, while optimal transmission power and sub-carrier allocation is accomplished by solving (23). Whereas the selection of active UAVs were carried out without considering the QoS constraint of users by using the formula $L = \lceil \frac{\lambda N}{K} \rceil$.
- *Equal Power Allocation:* This scheme employs the optimal sub-carrier allocation with an equal transmission power allocation to all users.
- *Random Sub-Carrier Allocation:* In this scheme, sub-carriers are allocated at random, while transmission power is allocated optimally.
- *Random Power:* This scheme allocates sub-carriers optimally while allocating transmission power randomly to ensure service quality for all users.
- *Joint Power and Bandwidth Allocation [4]:* In this scheme, A2G communication is carried out over an orthogonal frequency band to minimize inter-cell interference, while UE's sum rate is maximized by optimizing transmission power, bandwidth, and the 3D location of UAV's simultaneously.

Furthermore, we perform Monte Carlo simulations, and average results are produced over an independent channel.

A. Performance Analysis.

In Fig.3, the convergence of proposed algorithms is demonstrated and compared with different stimulation parameters. Fig.3a represents the convergence graph of Algorithm 1 by considering path loss as a performance matrix. Results reveal that as the number of iterations increases, the path loss of the

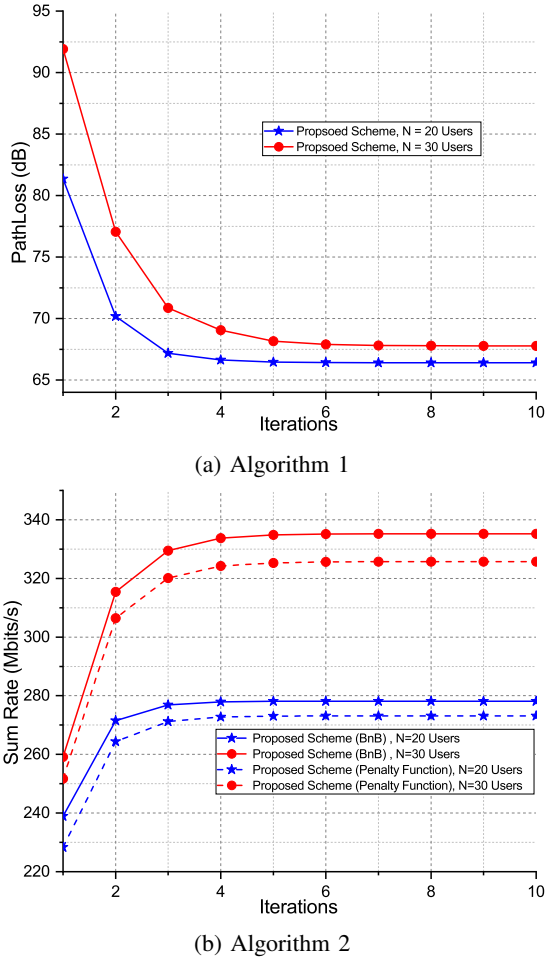


Fig. 3: Convergence Analysis of Algorithm 1 & Algorithm 2

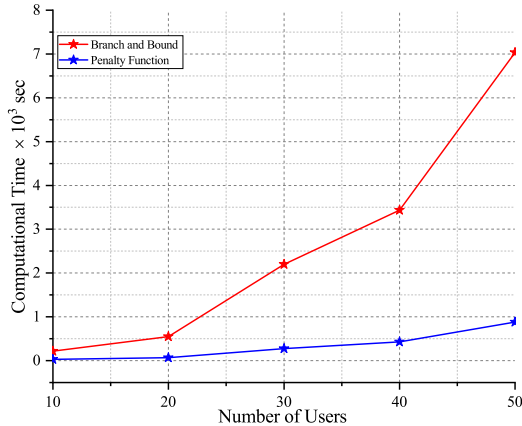


Fig. 4: Time Complexity

network also decreases. This trend is because UAVs update their locations and user association matrix incrementally. As a result, the distance between UAVs and associated users decreases, and path loss decreases as well. On the other hand, the convergence time for various simulation parameters tends to vary. As the number of users increases, more stimulation parameters are added to the system, requiring more computation to find a feasible solution that minimizes the path loss values.

Based on the UAV's optimal 3D locations and user association matrix solved by Algorithm 1, we solve the optimal resource allocation optimization problem using Algorithm 2. Results in Fig. 3b represent the convergence behaviour of both (23) and (25) in terms of sum rate as a performance matrix. Results reveal that the algorithm converges to a stable (feasible) point after some iterations.

Fig. 3b also confirms the effectiveness of the relaxed problem (25) compared with the mixed binary problem (23), which is revealed via an acceptable tolerance gap between two curves. Although having a slightly degraded performance, the relaxed problem (25) significantly reduces the computation time compared with the mixed binary problem (23), as shown in Fig. 4. For the small number of users, the time required to compute (23) and (25) is small. In contrast, the computational time required to solve the mixed binary problem grows exponentially with the number of users compared to the relaxed version.

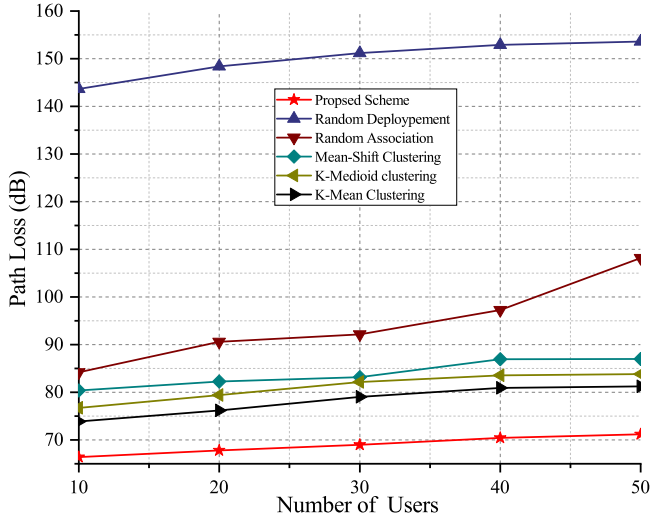
B. Pathloss and Sum Rate Performance

Because the system sum rate largely depends on the path loss between the UAV and its serving users, we evaluate both path loss and sum rate as the performance matrices of the proposed algorithms.

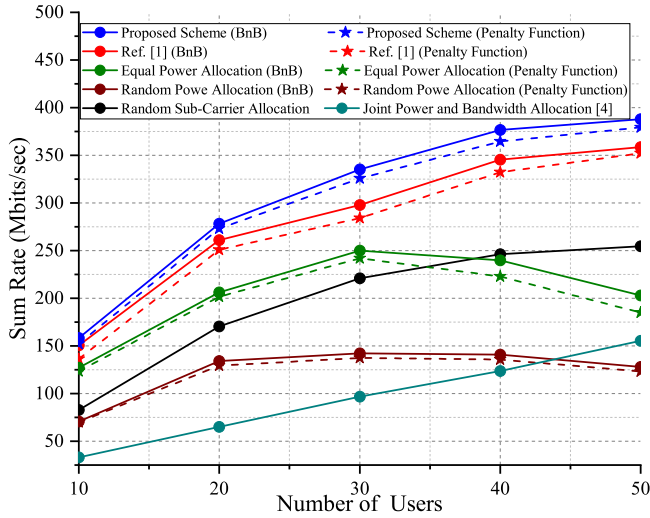
Fig. 5a represents the comparative analysis of the proposed scheme by considering path loss as a performance metric. The outcome reveals that the proposed scheme outperforms all other schemes. In our design, the optimal number of UAVs are selected and placed in the 3D cartesian coordinate system by considering the user QoS. Likewise, users are connected only to the UAV located at the closest distance compared to others.

Fig. 5b compares the sum rate of the proposed algorithm with other reference schemes as a function of the users. Superior performance is observed by the proposed algorithm compared with the reference solutions. Furthermore, results reveal a fundamental trade-off between optimal resource allocation and equal power allocation. Results demonstrate that for a small number of users, an equal power allocation scheme performs better than the optimal power allocation; on the other hand, as the number of users increases, the optimal power allocation scheme starts to perform better than others. This trend is because inter-cell interference also increases with the increase in the number of users; as a result, the sum rate starts decreasing in an equal power allocation scheme.

Similarly, in a UAV communication system, the probability of line-of-sight (ϕ) communication is a significant performance-influencing parameter. In practice, not all users have a line-of-sight communication link and have higher path loss than others, hence their QoS compromise. Whereas in our proposed scheme, the selection and deployment of UAVs are carried out by taking into account the QoS requirement of each user and the probability of line of sight, respectively. To analyze the impact, simulations are carried out for different values of ϕ , and $N = 20$ users are sorted in ascending order according to path loss as shown in Fig. 6. Results reveal that the sum rate increases as the number of users increases. On the



(a)



(b)

Fig. 5: Comparison of proposed solution

other hand, as there are users with NLoS links, the system sum rate starts decreasing. This trend is because more transmission power is required to satisfy these users' QoS requirements; hence, the sum rate decreases significantly. In the same way, results show that a higher probability of LoS communication results in a higher system sum rate.

To further reveal the proposed scheme's effectiveness, numerical results are compared with the Ref. [1], in which the number of UAVs is selected regardless of the user QoS requirements. The results of the Ref. [1] for different ϕ demonstrate that at $\phi = 95\%$, Ref. [1] can accommodate the number of non-line of sight users. In contrast, for $\phi = 85, 75\%$ number of non-line of sight users are more significant as compared to $\phi = 95\%$; hence UAVs do not have enough required transmission power to accommodate them; as a result, sum rate decrease significantly for $\phi = 85\%$ and goes to zero for $\phi = 75\%$ respectively. The proposed approach's significance in comparison to the theoretical minimum approach can be seen more explicitly by considering outage probability as

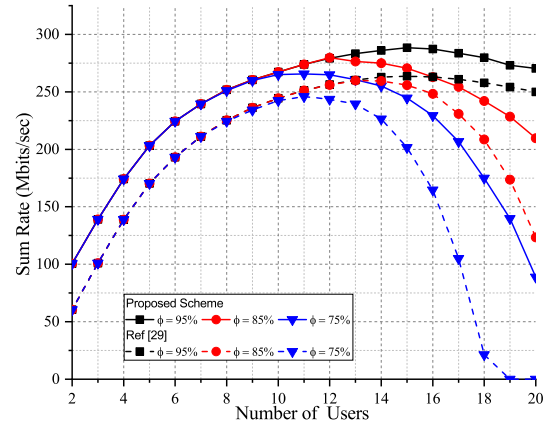


Fig. 6: Impact of the probability of line of sight on the system performance.

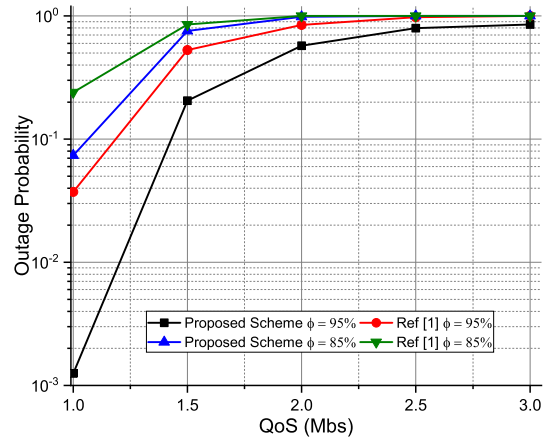
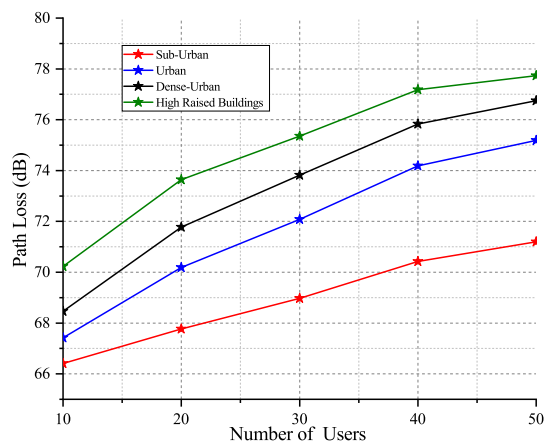


Fig. 7: Outage Probability

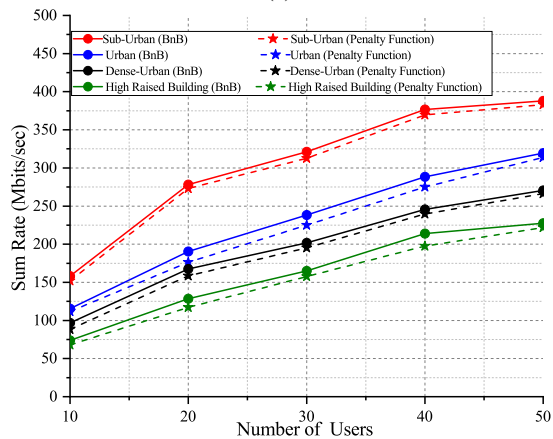
a performance metric across varying spectral efficiency, as shown in Fig. 7. The findings demonstrate the effectiveness of the proposed approach in comparison to others.

Similarly, simulations were carried out to further analyze the performance for path loss and sum rate problems in suburban, urban, dense-urban, and high-raised building environments. Results in Fig. 8a demonstrate that the sub-urban environment constitutes minimal path loss. On the other hand, as we move toward other working environments, values of the additional coefficient for path loss increase as given in Table I. Following that, the system's performance is further evaluated for the sum rate performance metric under different environments, as shown in Fig. 8b. Results reveal that the system sum rate is higher for a sub-urban working environment than others because of its minimal path loss. Similarly, Fig. 8 illustrates the working environment's impact on the system's performance.

Next, the proposed scheme performance is further validated by taking into account the UAV-UE connectivity and individual sum rate of different UAVs for $N=30$ as shown in Fig. 9. In particular, Fig. 9a shows UAV-UE connectivity, where the proposed scheme requires 5 UAVs to serve 30 UEs. According to the proposed scheme, UAVs are deployed optimally at a



(a)



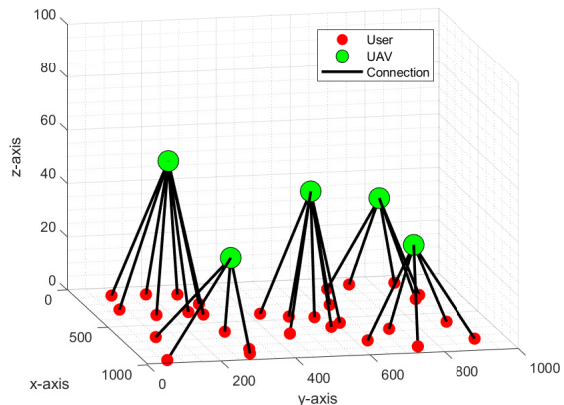
(b)

Fig. 8: Impact of working environment on the system performance.

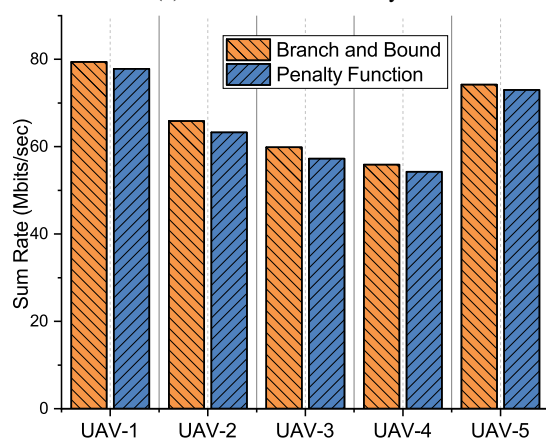
point such that the distance between UAVs and associated users is minimized. Moreover, the impact of the proposed association scheme can be seen in Fig.9b by plotting the sum rate of individual UAVs. It can be observed that our approach produces a load-balanced system configuration, and there is no significant deviation among the load of different UAVs.

V. CONCLUSIONS AND DISCUSSIONS

In this work, we have considered an ODFMA-enabled multiple UAV communication system to provide on-demand communication services in emergency scenarios. In this context, We formulate a novel problem to maximize the sum rate via a joint optimization of the number of active UAVs, their 3D placement, and the radio resource allocation under a limited transmit power budget and users' QoS requirements. Since the original optimization problem is not convex, we first decoupled it into sub-problems, which we then solved iteratively to find the best feasible solution. Furthermore, the effectiveness of the proposed scheme is illustrated via numerical results. Results demonstrate that the proposed scheme outperforms the benchmark schemes in terms of both path loss and user sum rate. We showed that optimal deployment and user association minimize path loss, directly impacting



(a) UAV-UE connectivity



(b) Rate per UAV

Fig. 9: UAV-UE connectivity and individual UAV rate for $N=30$.

the system sum rate. The results also demonstrated that by increasing the probability of the light-of-sight channel, the path loss decreases significantly, thereby improving the system sum rate.

The outcomes of this work suggest several promising research topics. The first topic is to consider the user dynamic, in which the number of users is time-varying. In such cases, the number of active UAVs should be planned jointly with the prediction of active users. The second topic is studying the UAV movement in the deployment design. This may reduce the number of active UAVs; however, the problem will be more challenging.

APPENDIX A PROOF OF LEMMA 1

We can prove the expressions \mathbf{H}_o , \mathbf{H}_n , \mathbf{F}_o , \mathbf{F}_n , κ_o and κ_n by considering the objective function and constraints of (15), which are represented by f_1 and f_2 respectively:

$$f_1(\mathbf{W}) = \sum_{n=1}^{Q^l} [(x_n - x_l)^2 + (y_n - y_l)^2 + h_l^2], \forall l. \quad (26)$$

$$f_2(\mathbf{W}) = (x_n - x_l)^2 + (y_n - y_l)^2 + h_l^2 \xi \leq 0. \quad (27)$$

In (16), \mathbf{H}_o , and \mathbf{H}_n represent the positive semi-definite matrices that can be calculated by using the second partial derivatives of f_1 and f_2 , respectively. As a result, the Hessian of $f_1(\mathbf{W})$ and $f_2(\mathbf{W})$ can be defined as follows:

$$\mathbf{H}_o = \nabla^2 f_1(\mathbf{W}) = \begin{bmatrix} 2Q^l & 0 & 0 \\ 0 & 2Q^l & 0 \\ 0 & 0 & 2Q^l \end{bmatrix} = 2Q^l \mathbf{I}_3. \quad (28)$$

$$\mathbf{H}_n = \nabla^2 f_2(\mathbf{W}) = \begin{bmatrix} 2 & 0 & 0 \\ 0 & 2 & 0 \\ 0 & 0 & \xi \end{bmatrix}. \quad (29)$$

Equation (28) and (29) represents the Hessian matrix of f_1 and f_2 , whose all the elements are zeros except the diagonal elements such that $|\nabla^2(f_1(\mathbf{W}))| > 0$ and $|\nabla^2(f_2(\mathbf{W}))| > 0$. As a result, the objective function and constraints **C1** specified in (15) are convex in nature.

Following that, the transformation from (15) to (16) can be proven by simply expanding and rearranging the quadratic terms in (26) and (27) in the following manner:

$$f_1(\mathbf{W}) = \underbrace{\sum_{n=1}^{Q^l} (x_n^l + y_n^l + h^l)^2}_{\text{OT1}} + \underbrace{\sum_{n=1}^{Q^l} (-2x_n x^l - 2y_n y^l)}_{\text{OT2}} + \underbrace{\sum_{n=1}^{Q^l} (x_n^2 + y_n^2)}_{\text{OT3}}. \quad (30)$$

Similarly,

$$f_2(\mathbf{W}) = \underbrace{(x^l + y^l + \xi h^l)^2}_{\text{CT1}} + \underbrace{(-2x_n x^l - 2y_n y^l)}_{\text{CT2}} + \underbrace{(x_n^2 + y_n^2)}_{\text{CT3}}. \quad (31)$$

To prove the transformation of (15a) to (16a), we start solving (30) and find the value of OT1, OT2 and OT3 respectively. As perceived from (30) we have

$$\text{OT1} = \sum_{n=1}^{Q^l} (x_n^l + y_n^l + h^l)^2, \quad (32)$$

whereas $x^l + y^l + h^l$ in matrix notation can be represented as follows:

$$x^l + y^l + h^l = \begin{bmatrix} x^l \\ y^l \\ h^l \end{bmatrix}^T \begin{bmatrix} 1 & 0 & 0 \\ 0 & 1 & 0 \\ 0 & 0 & 1 \end{bmatrix} \begin{bmatrix} x^l \\ y^l \\ h^l \end{bmatrix} = \mathbf{W}^T \mathbf{I}_3 \mathbf{W}, \quad (33)$$

Putting the value of (33) in (32), we have

$$\text{OT1} = \sum_{n=1}^{Q^l} \mathbf{W}^T \mathbf{I}_3 \mathbf{W} = \mathbf{W}^T Q^l \mathbf{I}_3 \mathbf{W}, \quad (34)$$

Whereas, from (28), $Q^l \mathbf{I}_3 = \frac{1}{2} \mathbf{H}_o$ and by putting the value in (34), we have

$$\text{OT1} = \frac{1}{2} \mathbf{W}^T \mathbf{H}_o \mathbf{W}. \quad (35)$$

Similarly from (30), OT2 in matrix notation can be represented as follows:

$$\text{OT2} = \sum_{n=1}^{Q^l} (-2x_n x^l - 2y_n y^l) = \underbrace{\begin{bmatrix} -2 \sum_{n=1}^{Q^l} x_n \\ -2 \sum_{n=1}^{Q^l} y_n \\ 0 \end{bmatrix}^T}_{\mathbf{F}_o} \begin{bmatrix} x^l \\ y^l \\ h^l \end{bmatrix} = \mathbf{F}_o^T \mathbf{W}. \quad (36)$$

Similarly from (30), OT3 represented as

$$\text{OT3} = \sum_{n=1}^{Q^l} (x_n^2 + y_n^2) = \kappa_o. \quad (37)$$

Following the same procedure, we find the value of CT1 = $\frac{1}{2} \mathbf{W}^T \mathbf{H}_n \mathbf{W}$, CT2 = $\mathbf{F}_n^T \mathbf{W}$ and CT3 = $\kappa_n = x_n^2 + y_n^2$.

Putting the value of OT1, OT2 and OT3 in (30) and CT1, CT2 and CT3 in (31) we have $f_1(\mathbf{W}) = \frac{1}{2} \mathbf{W}^T \mathbf{H}_o \mathbf{W} + \mathbf{F}_o^T \mathbf{W} + \kappa_o$ and $f_2(\mathbf{W}) = \frac{1}{2} \mathbf{W}^T \mathbf{H}_n \mathbf{W} + \mathbf{F}_n^T \mathbf{W} + \kappa_n$, which completes the proof.

REFERENCES

- [1] A. Mahmood, T. X. Vu, S. K. Sharma, S. Chatzinotas, and B. Ottersten, "Multi-objective optimization for 3d placement and resource allocation in ofdma-based multi-uav networks," *arXiv preprint arXiv:2304.12798*, 2023.
- [2] A. A. Khuwaja *et al.*, "Optimum deployment of multiple UAVs for coverage area maximization in the presence of co-channel interference," *IEEE Access*, vol. 7, pp. 85 203–85 212, 2019.
- [3] R. I. Bor-Yaliniz *et al.*, "Efficient 3-D placement of an aerial base station in next generation cellular networks," in *2016 IEEE International Conference on Communications (ICC)*, 2016, pp. 1–5.
- [4] P. Li and J. Xu, "Placement optimization for UAV-enabled wireless networks with multi-hop backhauls," *Journal of Communications and Information Networks*, vol. 3, no. 4, pp. 64–73, 2018.
- [5] A. Masaracchia *et al.*, "An energy-efficient clustering and routing framework for disaster relief network," *IEEE Access*, vol. 7, pp. 56 520–56 532, 2019.
- [6] O. Kodheli *et al.*, "Satellite communications in the new space era: A survey and future challenges," *IEEE Communications Surveys & Tutorials*, vol. 23, no. 1, pp. 70–109, 2021.
- [7] E. Kalantari *et al.*, "On the number and 3D placement of drone base stations in wireless cellular networks," in *2016 IEEE 84th Vehicular Technology Conference (VTC-Fall)*, 2016, pp. 1–6.
- [8] Y. Zeng *et al.*, "Accessing from the sky: A tutorial on UAV communications for 5G and beyond," *Proceedings of the IEEE*, vol. 107, no. 12, pp. 2327–2375, 2019.
- [9] M. Mozaffari *et al.*, "A tutorial on UAVs for wireless networks: Applications, challenges, and open problems," *IEEE Communications Surveys Tutorials*, vol. 21, no. 3, pp. 2334–2360, 2019.
- [10] M. Mozaffari *et al.*, "Drone small cells in the clouds: Design, deployment and performance analysis," in *2015 IEEE Global Communications Conference (GLOBECOM)*, 2015, pp. 1–6.
- [11] Y. Liang *et al.*, "Joint trajectory and resource optimization for UAV-aided two-way relay networks," *IEEE Transactions on Vehicular Technology*, vol. 71, no. 1, pp. 639–652, 2022.
- [12] L. Xie, J. Xu, and R. Zhang, "Throughput maximization for UAV-enabled wireless powered communication networks," *IEEE Internet of Things Journal*, vol. 6, no. 2, pp. 1690–1703, 2019.
- [13] G. Zhang, Q. Wu, M. Cui, and R. Zhang, "Securing UAV communications via joint trajectory and power control," *IEEE Transactions on Wireless Communications*, vol. 18, no. 2, pp. 1376–1389, 2019.
- [14] S. Zeng *et al.*, "Trajectory optimization and resource allocation for ofdma UAV relay networks," *IEEE Transactions on Wireless Communications*, vol. 20, no. 10, pp. 6634–6647, 2021.
- [15] M. Alzenad *et al.*, "3-D placement of an unmanned aerial vehicle base station (UAV-bs) for energy-efficient maximal coverage," *IEEE Wireless Comm. Letters*, vol. 6, pp. 434–437, 2017.
- [16] C. You and R. Zhang, "3D trajectory optimization in rician fading for UAV-enabled data harvesting," *IEEE Transactions on Wireless Communications*, vol. 18, no. 6, pp. 3192–3207, 2019.
- [17] F. Huang *et al.*, "Multiple-UAV-assisted swipt in internet of things: User association and power allocation," *IEEE Access*, vol. 7, pp. 124 244–124 255, 2019.
- [18] L. Xie *et al.*, "Common throughput maximization for UAV-enabled interference channel with wireless powered communications," *IEEE Transactions on Communications*, vol. 68, no. 5, pp. 3197–3212, 2020.
- [19] Z. Rahimi *et al.*, "An efficient 3-D positioning approach to minimize required UAVs for iot network coverage," *IEEE Internet of Things Journal*, vol. 9, no. 1, pp. 558–571, 2022.
- [20] R. Chen, X. Li, Y. Sun, S. Li, and Z. Sun, "Multi-UAV coverage scheme for average capacity maximization," *IEEE Communications Letters*, vol. 24, no. 3, pp. 653–657, 2020.
- [21] J. G. Andrews *et al.*, "What will 5G be?" *IEEE Journal on Selected Areas in Comm*, vol. 32, no. 6, pp. 1065–1082, 2014.
- [22] X. Liu *et al.*, "Trajectory design and power control for multi-UAV assisted wireless networks: A machine learning approach," *IEEE Tran. on Vehicular Technology*, vol. 68, pp. 7957–7969, 2019.

- [23] H. El Hammouti, M. Benjillali, B. Shihada, and M.-S. Alouini, "Learn-as-you-fly: A distributed algorithm for joint 3D placement and user association in multi-uavs networks," *IEEE Transactions on Wireless Communications*, vol. 18, no. 12, pp. 5831–5844, 2019.
- [24] A. Al-Hourani *et al.*, "Modeling air-to-ground path loss for low altitude platforms in urban environments," in *2014 IEEE Global Communications Conference*, 2014, pp. 2898–2904.
- [25] C. Lu, S.-C. Fang, Q. Jin, Z. Wang, and W. Xing, "KKT solution and conic relaxation for solving quadratically constrained quadratic programming problems," *SIAM Journal on Optimization*, vol. 21, no. 4, pp. 1475–1490, 2011.
- [26] M. S. Lobo, L. Vandenberghe, S. Boyd, and H. Lebret, "Applications of second-order cone programming," *Linear algebra and its applications*, vol. 284, no. 1-3, pp. 193–228, 1998.
- [27] A. Beck *et al.*, "A sequential parametric convex approximation method with applications to nonconvex truss topology design problems," *Journal of Global Optimization*, vol. 47, no. 1, pp. 29–51, 2010.
- [28] T. S. Abdu *et al.*, "Flexible resource optimization for GEO multibeam satellite communication system," *IEEE Transactions on Wireless Communications*, vol. 20, no. 12, pp. 7888–7902, 2021.
- [29] T. X. Vu *et al.*, "Dynamic bandwidth allocation and precoding design for highly-loaded multiuser MISO in beyond 5G networks," *IEEE Transactions on Wireless Communications*, vol. 21, no. 3, pp. 1794–1805, 2022.